

# 5 The urban heat island effect in Dutch city centres – Identifying relevant indicators and first explorations

*Article 4 The Urban Heat Island Effect in Dutch city centres – Identifying relevant indicators and first explorations. Published in W. Leal et al. (eds.), Implementing Climate Change Adaptation in Cities and Communities, Climate Change Management, DOI 10.1007/978-3-319-28591-7\_7, © Springer International Publishing Switzerland 2016*

Leyre Echevarría Icaza<sup>1\*</sup>, Frank van der Hoeven<sup>2</sup> and Andy van den Dobbelsteen<sup>3</sup>

1 Delft University of Technology. Faculty of Architecture and the Built Environment. Address: Julianalaan 134, 2628 BL Delft, The Netherlands; E-Mail: L.EchevarriaIcaza@tudelft.nl

2 Delft University of Technology. Faculty of Architecture and the Built Environment. Address: Julianalaan 134, 2628 BL Delft, The Netherlands; E-Mail: F.D.vanderHoeven@tudelft.nl

3 Delft University of Technology. Faculty of Architecture and the Built Environment. Address: Julianalaan 134, 2628 BL Delft, The Netherlands; E-Mail: a.a.j.f.vandendobbelsteen@tudelft.nl

\* Author to whom correspondence should be addressed; E-Mail: L.EchevarriaIcaza@tudelft.nl; Tel.: +34 619 80 32 71

## Abstract

---

In the Netherlands awareness regarding the Urban Heat Island (UHI) was raised relatively recently. Because of this recent understanding, there is a lack of consistent urban micro-meteorological measurements to allow a conventional UHI assessment of Dutch cities during heat waves. This paper argues that it is possible to retrieve relevant UHI information – including adaptation guidelines – from satellite imagery.

The paper comprises three parts. The first part consists of a study of suited indicators to identify urban heat islands from which a method is presented based on ground heat flux mapping. The second part proposes heat mitigation strategies and identifies the areas where these strategies could be applied within the hotspots identified in the cities of The Hague, Delft, Leiden, Gouda, Utrecht and Den Bosch. The third part estimates the reduction of urban heat generated by the increase of roof albedo in the hotspots of the six cities. The six cities hotspots are located within the boundaries of the 17th century city centres. In order to avoid interference with cultural values of these

historical environments most likely UHI mitigation measures regard improving the thermal behaviour of the city roofs. For instance, applying white coatings on bitumen flat roofs (or replacing them by white single-ply membranes) and replacing sloped roof clay tiles by coloured tiles with cool pigments can reduce the urban heat hotspots by approximately 1.5°C.

Remote sensing provides high level information that provide urban planners and policy makers with overall design guidelines for the reduction of urban heat.

**Keywords:** Climate Change, Urban Heat Island, Storage Heat Flux, Remote Sensing, Climate Adaptation, NDVI, Albedo

---

## § 5.1 Introduction

---

### § 5.1.1 UHI studies despite the lack of micro-measurements

---

According to the Royal Netherlands Meteorological Institute (KNMI) 33 heat waves have struck the Netherlands since the beginning of the 19th century (KNMI, 2014). Nevertheless, Dutch urban meteorologists only started to study the Urban Heat Island (UHI) phenomenon after the heat wave of 2003, when the amount of heat-related deaths reached more than 1,400 (Garssen et al., 2005) in the Netherlands and more than 22,000 across Europe (Schar & Jendritzky, 2004). In the Netherlands, this relatively recent awareness of the phenomenon explains the lack of historical air temperature records to allow a consistent analysis of the UHI patterns throughout the country (Hove et al., 2011). Future climate scenarios predict that the frequency, the intensity and the duration of heat waves will increase (Meehl et al., 2004), more specifically in the Netherlands the four climate scenarios predicted for 2050 by the KNMI forecast that the average summer temperatures in the rural environment will continue to rise, and so will the amount of ‘summerly days’ (maximum temperature above or equal to 25°C) per year in the rural environment across the country. Concerned by these future predictions, Dutch scientists, climatologists and urban planners have had to develop alternative ways to fill in the shortage of historical urban air temperature records, in order to study more in depth the phenomenon in different Dutch cities. Some have used hobby meteorologist’s data (Hove et al., 2011; Steeneveld et

al., 2011; Koopmans S. 2010), others have used cargo bicycles (Heusinkveld et al., 2010; Brandsma et al., 2012) to retrieve temperature variations through different cities during hot summer days and finally others have chosen to use satellite imagery to map land surface temperature variations during hot days (Hoeven et al., 2013; Klok et al. 2009).

### § 5.1.2 Bridging the gap between scientific and applied knowledge

---

Even though in the Netherlands the scientific community has started investigating the phenomenon already more than five years ago, it seems there is still a gap between the scientific knowledge developed and the urban policies of large and medium size cities, which haven't started implementing measures to mitigate urban heat yet. Precisely one of the goals of the research programme Knowledge for Climate (Knowledge For Climate, 2015) is to develop not only scientific but also applied knowledge for climate proofing the Netherlands, investigating a wide variety of topics ranging from the climate adaptation for rural areas (Climate Adaptation for Rural Areas, 2015) to the climate adaptation of cities (Climate Proof Cities, 2014), to which this study belongs. Many Dutch cities have taken part in the Climate Proof Cities Program either as stakeholders or as case cities and would be willing to implement measures to mitigate the urban heat problem however they often lack a basic overview of the most affected neighbourhoods (to identify the areas where to concentrate the urban heat mitigation efforts), the different mitigation options (to be able to select design mitigation proposals that match best the rest of urban planning priorities) and a high level estimation of the potential heat reduction achieved (to be able to quantify the mitigation effect).

### § 5.1.3 Remote sensing as a tool to identify, mitigate and quantify urban heat.

---

For this study the authors have chosen to use satellite imagery because on the one hand it allows mapping and analysing many heat related parameters, such as surface heat fluxes (Parlow, 2003), land surface temperatures (Dousset, 2011), albedo (Taha, 1997; Sailor 1997) vegetation indexes (Yuan et al., 2007; Gallo et al., 1993) and on the other hand the analysis of satellite imagery provides consistent information of several cities at the same time. Being able to analyse several heat related parameters

allows not only to identify vulnerable areas within cities, but also to assess on the different potential mitigation strategies for each city analysed and to provide a high level quantification of surface materials. The possibility of producing a simultaneous analysis of several comparable cities allows the analysed cities to join efforts, share scientific knowledge and implementation strategies. In this study the cities of The Hague, Delft, Leiden, Gouda, Utrecht and Den Bosch (Figure 5.1 and Figure 5.2) were analysed. These cities have in common that they have a dense historical inner-city, dating back to medieval times but mostly consisting of buildings from the seventeenth century, the 'Golden Age' of the Netherlands, when most cities expanded rapidly with stone building that often still remain. Thanks to this comparable past and development, the chosen cities are comparable, although their urban layout and recent alterations differ.

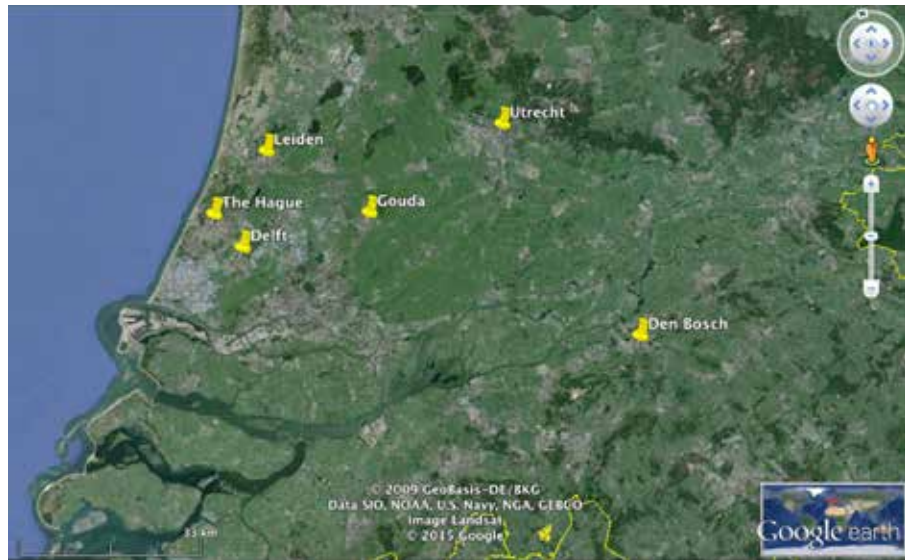


FIGURE 5.1 Analysed cities. Google earth image. Data SIO, NOAA, U.S. Navy, NGA, GEBCO ©2015Google. Image Landsat ©2009 GeoBasis-DE/BKG

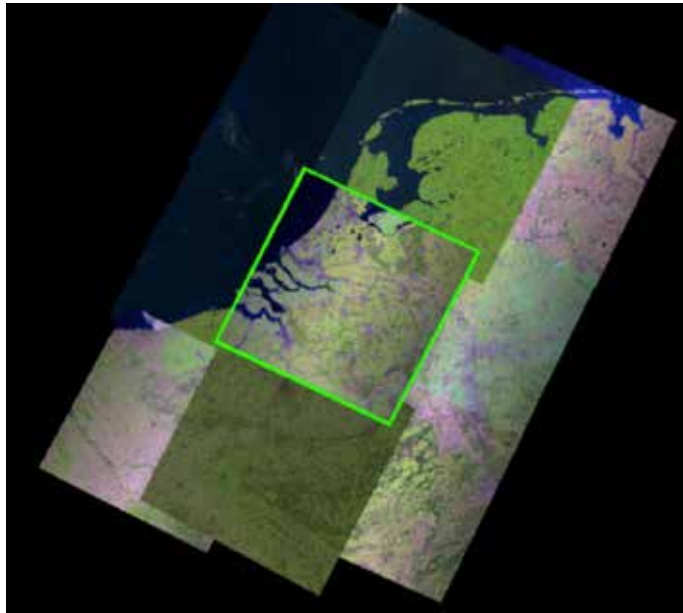


FIGURE 5.2 Size of the Landsat 5 TM image analysed.(image extracted from the USGS Global Visualization Viewer). Courtesy of the U.S. Geological Survey. USGS/ NASA Landsat.

---

## § 5.2 Methodology

---

### § 5.2.1 Research framework

---

- Problem statement and objective

Since in the Netherlands UHI awareness is relatively recent, there is a lack of consistent urban micro-meteorological measurements to allow a conventional and consistent UHI assessment of Dutch cities during heat waves (Hove et al., 2011). This lack of appropriate data hampers UHI scientific studies and hinders the development of guidelines for climate adaptation in cities. Therefore, as part of this study the authors

aim to retrieve relevant UHI information from satellite imagery, in order to help develop UHI adaptation guidelines for Dutch cities.

The objective of this study is twofold: to develop a method to assess the UHI phenomenon for cities with a lack of micro-meteorological datasets, and to develop a customised set of urban planning adaptation measures for the studied cities.

- Research questions: The underlying research questions for this paper are:
  - Can remote sensing help identify urban heat hotspots when there is lack of micro-measurements? If so, what are suited indicators?
  - Which are the most common heat mitigation strategies to reduce urban heat? How can we use remote sensing to identify where to implement these within the hotspots identified for the cities of The Hague, Delft, Leiden, Gouda, Utrecht and Den Bosch?
  - Could we quantify the mitigation effect of the increase of roof albedo in the identified hotspots?

## § 5.2.2 Research methodology

---

- Research structure

Based on the research questions this paper primarily comprised three parts.

The first part consists of a study of suited indicators to identify urban heat hotspots in areas with a lack of micro-measurements, from which a method is presented based on storage heat flux mapping. This was validated by application in 2 Dutch cities, The Hague and Utrecht.

The second part proposes heat mitigation strategies and identifies the areas where these heat mitigations could be applied within the hotspots identified in the cities of The Hague, Delft, Leiden, Gouda, Utrecht and Den Bosch. The third part estimates the reduction of urban heat generated by the increase of albedo in the hotspots of the six cities.

- Data collection instruments

Landsat 5 TM satellite imagery was used for the assessment of the tree parts of the research. Landsat is often used for UHI assessment (Bechtel, 2011; Liu and Zhang,

2011; Rajasekar and Weng, 2009; Cao et al., 2008), for the development of mitigation strategies (Rosenzweig et al., 2006; Baudouin Y. and Lefebvre S. 2014) or for the estimation of the heat mitigation effect (Odindi et al. 2015; Onishi et al. 2010). Landsat imagery has a high resolution and is open source. The raw satellite images can be downloaded from the US Geological Survey (USGS) webpage, Earth Resources Observation and Science Center (EROS). The approximate size of each retrieved scene is 170 km North-South by 183 km East-West. One Landsat image covers most of the country surface, which allows completing the simultaneous analysis of several cities at the same time (fig. 1b.). The sensor carried onboard Landsat 5 is Landsat Thematic Mapper (TM) which has a 16 day repeat circle. For this study the autho chose to analyse satellite images retrieved during the second heat wave that struck The Netherlands in 2006 (on the 16th of July at 10:33 UTC for all cities, except for Den Bosch, for which the Landsat image used was from the 25th of July, at 10:26 UTC).

Two software have been used to process the raw satellite imagery: ATCOR 2/3 and ENVI 4.7. ATCOR 2/3 was used for the atmospheric and geometric correction of the satellite imagery, as well as for the production of the albedo and surface heat flux maps (Richter & Schlapfer, 2013) and ENVI 4.7 (Exelisvis, 2015) was used for the analysis and enhancement of the images processed in ATCOR 2/3.

– Identifying hotspots

For the selected cities urban heat island hotspots were mapped by means of the storage heat flux. The storage heat flux was mapped using ATCOR 2/3 (Figure 5.3).

Analytical phases	Scale	Parameter analysed	Methods and tools	Design guidelines
<b>Phase 1</b>				
Hotspot identification	City	Storage heat flux	Landsat 5 TM for July 2006. Geometrical correction, atmospherical correction and <b>Storage heat flux</b> calculation for urban environment in ATCOR 2/3.	Definition of intervention area.

FIGURE 5.3 Hotspot identification process

The calculation of the heat fluxes is done through different models for urban and rural surfaces. In order to identify the hotspots (areas with the highest storage heat flux values) within the studied cities, the authors have chosen to use the model used for urban surfaces, where latent heat is usually smaller. The dominant fluxes are the storage and the sensible heat fluxes, for which Parlow's equations are applied (Parlow, 1998).

#### FORMULA 5.1

$$G = 0,4 R_n$$

where  $R_n$  is the net radiant energy absorbed by the surface;  $G$  is the storage heat flux, i.e. the energy dissipated by conduction into the ground or into the building materials

#### FORMULA 5.2

$$LE = 0,15 (R_n - G)$$

where  $R_n$  is the net radiant energy absorbed by the surface;  $G$  is the storage heat flux, i.e. the energy dissipated by conduction into the ground or into the building materials; and  $LE$  is the latent heat flux, that is the energy available of evapotranspiration.

#### FORMULA 5.3

$$H = R_n - G - LE$$

where  $R_n$  is the net radiant energy absorbed by the surface;  $G$  is the storage heat flux, i.e. the energy dissipated by conduction into the ground or into the building materials;  $H$  is the sensible heat flux, that is the energy dissipated by convection into the atmosphere (its behaviour varies depending on whether the surface is warmer or colder than the surrounding air); and  $LE$  is the latent heat flux, that is the energy available of evapotranspiration.

#### – Heat mitigation strategies

The analysis of remote sensing imagery can provide an overview of several urban heat related parameters: normalised difference vegetation index (NDVI), land surface temperature (LST), coolspot presence, and albedo (Figure 5.4). In this section an overview of the relevance of each of these parameters is provided. However, since in

five of the six analysed cities the “storage heat flux hotspots” are within the limits of the 17th century city centres – and in these areas the implementation of design strategies is fairly restricted due to the historical protection of the neighbourhoods – in the following sections the authors have only estimated the effect on the urban heat reduction of the mitigation strategies consisting of increasing the city roofs’ albedo.

Analytical phases	Scale	Parameter analysed	Methods and tools	Design guidelines
<b>PHASE 2</b>				
Adaptation measures	City	Cool Corridors	Coolspot identification; LandSat 5 TM for July 2006. Geometrical correction, atmospheric correction and Storage heat flux for rural environment calculation in AICOR 2.3. Wind corridor identification through ANNs.	1/Creation of cool wind corridors connecting hotspots to natural coolspots. 2/Enhancement and preservation of the existing coolspot.
	Hotspot	Albedo	LandSat 5 TM for July 2006. Geometrical and atmospheric correction and Albedo calculation in AICOR 2.3.	Proposal of surface material changes to improve albedo, depending on existing surface materials.
	Hotspot	NDVI	LandSat 5 TM for July 2006. Geometrical and atmospheric correction in AICOR 2.3. NDVI calculation in ENVI 4.7.	Vegetation introduction in highlighted hotspots.
	Hotspot	Land Surface Temperature	LandSat 5 TM for July 2006. LST calculation in ENVI 4.7.	In industrial areas, deeper analysis is required to confirm the energy efficiency of the buildings with high LST on roofs.

FIGURE 5.4 UHI adaptation measures recapitulation chart

#### – UHI reduction potentials

In order to estimate the UHI reduction for the six cities the implementation of the roof mitigation strategies was studied. These concern the measures that will be most likely adopted. The following methodology was adopted: the albedo maps of each hotspot were used to estimate the area of bituminous flat roofs and of clay tile sloped roofs. This area estimation was calculated using ENVI 4.7. For the estimation of the bituminous flat roofs, the authors considered all surfaces with albedos of 0.13 to 0.15, and for the clay tile surface estimation they considered all surfaces with albedos of 0.18 to 0.22. This way of estimating material surfaces has its limitations.

#### – Detailed assumptions

The following reference-based assumptions were used:

It was assumed that an increase of 0.1 of the hotspot overall albedo reduces the UHI by 1°C (Sailor, 1995; Taha, 1988).

As a reference, the maximum UHI values for the 95 percentile were provided, calculated with hobby meteorologists’ data (Hove et al., 2011) for the cities of The

Hague, Delft and Leiden. For the cities of Gouda, Utrecht and Den Bosch, it was estimated that the max UHI will be around 5°C as well.

For each city the authors have estimated the UHI reduction for several roof intervention scenarios:

- Mitigation action 1:

Bituminous flat roof albedo (0.13 to 0.15) is improved by applying a white coating (albedo 0.7) or by replacing it by a white single-ply membrane (albedo 0.7). This action is likely to take place in the next 10 years. Minor repairs can be treated with white coating solutions, and major repairs will require full replacement by single ply membranes.

- Mitigation action 2:

Clay tiles sloped roof (albedo 0.18 to 0.22) are replaced by coloured tiles with cool pigments (albedo 0.5). This action is likely to take place in the coming 50 years as the lifespan of clay tiles is 50 years.

- Mitigation action 1+2:

Consists in improving the albedo of bituminous flat roofs by applying a white coating or a single-ply membrane, and in improving the clay sloped roof albedo by cool pigment coloured tiles.

- Limitations

Landsat 5TM is an appropriate tool to assess urban heat accumulation at city scale (sections 5.3 and 5.4) due to the resolution of its spectral bands: 30m for bands 1 to 7, and 120m for band 6 which is resampled to 30m. However, in this study the authors have also used Landsat 5 TM to quantify the surface of bituminous flat roof and of clay sloped roofs (section 5.6). The resolution of Landsat 5TM for material discrimination is a little rough. Nonetheless, the purpose of the surface estimations is to provide a high-level quantification of the mitigation effect of the proposed measures, therefore a certain degree of inaccuracy in the surface quantification is acceptable. Further, the objective of the study is not only to quantify the mitigation effect of the measures, but also to suggest a methodology that could also be replicated with finer resolution satellite imagery, allowing more accurate surface classification results.

---

## § 5.3 Identification of UHI hotspots in areas with a lack of micro-measurements

---

### § 5.3.1 Possible UHI indicators

---

- UHI and SUHI

The most common variable assessed through remote sensing imagery is land surface temperature (LST). However, LST assesses the surface heat island (SUHI) phenomenon, which has different characteristics than the canopy layer air temperature urban heat island (UHI).

The first important difference between SUHI and UHI is that, even though both present higher intensities on cloudless and windless days (Oke 1973; Oke 1982; Uno et al., 1988; Morris et al., 2001) SUHI has its peak during the day when the surfaces receive the maximum radiation (Carlson et al., 1981), whereas the canopy UHI has its peak at night when the surfaces start radiating the stored energy into the atmosphere (Oke et al., 1997).

The second difference is that diurnal SUHI pattern does not match the nocturnal UHI pattern (Dousset et al., 2011; Parlow, 2003; Voogt et al., 2002; Roth et al., 1989; Price, 1979). Urban planners and climatologists are typically more interested in understanding nocturnal air temperature UHI patterns because they are more strongly connected to the accumulation of heat and to human comfort; there is a high correlation between high nocturnal temperatures and excess of mortality during heat waves (Dousset et al., 2011).

- Night-time UHI

Some studies suggest that the nocturnal surface temperatures are better correlated to nocturnal air temperatures than diurnal ones, due to the stabilization of the atmosphere and to the cessation of the direct solar radiation (Nichol & Wong, 2004). The reality is that most remote sensing studies on the UHI phenomenon focus on the day-time surface temperature variations due to the lack of fine resolution night-time thermal images. High-frequency thermal sensors that allow retrieving both day-time and night-time surface temperature typically have low resolutions (AVHRR: 1.1 km, Modis: 1 km) whereas finer resolution satellites such as Landsat TM (120 m) and

Landsat ETM (60 m) have lower frequencies and are therefore limited to day-time observations (Nichol & Wong, 2004). Thus finer resolution satellites mainly allow the retrieval of day-time LST which cannot be considered as the most relevant UHI indicator.

- Heat fluxes

Studies carried out in Basel by Parlow reveal that heat fluxes might be more relevant indicators of the UHI phenomenon than day-time surface temperature patterns (Parlow, 2003). Therefore in this study remote sensing imagery is therefore used as a basis for mapping heat fluxes, more precisely storage heat fluxes.

The energy balance equation for radiant energy absorbed by heat fluxes can be written as (Asrar, 1989):

#### FORMULA 5.4

$$R_n = G + H + LE$$

where  $R_n$  is the net radiant energy absorbed by the surface;  $G$  is the storage heat flux, i.e. the energy dissipated by conduction into the ground or into the building materials;  $H$  is the sensible heat flux, that is the energy dissipated by convection into the atmosphere (its behaviour varies depending on whether the surface is warmer or colder than the surrounding air); and  $LE$  is the latent heat flux, that is the energy available of evapotranspiration.

- Storage heat flux as indicator of UHI

Studies on heat storage of paved surfaces in urban areas reveal that these may be the principal contributor to the nightly UHI effect (Doll et al., 1985). Net radiation, storage heat flux, latent heat and sensible heat distribution vary in the urban and rural environments. Studies on the 'Urban Energy Balance' derived from satellite data for the city of Basel (Parlow, 2003) reveal that during day-time, urban pavements, industrial pavements and roofs present low latent heat fluxes, sensible heat fluxes similar to the ones obtained in their rural surroundings (among other reasons, due to the high surface temperatures of the urban surfaces) and extremely high storage heat fluxes. The heat accumulated during the day is released to the atmosphere during the night thus causing the UHI peak. Materials with higher conductivity – such as black top concrete and asphalt – present lower surface temperatures during the day, however at night – due to the different heat storage capacity of the two materials – black top

concrete presented higher surface temperatures than the asphalt pavement (Asaeda et al., 1993). Therefore, storage heat flux proves to be a relevant indicator for the UHI assessment. Urban areas present higher temperatures at night due to thermal conductivity, heat capacity and thermal admittance of the built materials (Parlow, 2003). Furthermore, other studies confirm that the data modelled with remote sensing imagery is in agreement with the micrometeorological in-situ measurements. (Rigo & Parlow, 2007).

- Practical storage heat flux values

As a reference, the urban areas of Mulhouse and Basel, as well as their industrial sites, present storage heat fluxes of more than 200 W/m<sup>2</sup>, whereas the forest areas present values of 26 to 50 W/m<sup>2</sup> (Parlow, 2003). Other storage heat flux values per surface types are compiled in the ATCOR-2/3 User Guide (Version 8.0.2), which to dark asphalt areas assigns storage heat flux values of 240 W/m<sup>2</sup>, to bright concrete values ranging from 164 to 240 W/m<sup>2</sup>, to partially vegetated areas values of 185 W/m<sup>2</sup> and to fully vegetated areas values of 77 W/m<sup>2</sup> (Richter & Schlapfer, 2013).

---

## § 5.4 Validation examples: comparing storage heat flux mapping with multi-day mobile observations for the cities of The Hague and Utrecht

---

### § 5.4.1 The Hague

---

Although there is a lack of ground measurements during heat waves, some research groups have attempted to map the UHI hotspots through other methods. This is the case for the maps issued by De Groot (2011), which for the city of The Hague forecasts the number of nights with temperatures above 20°C for the 2050 KNMI climate scenarios W and W+ (KNMI, 2009). These maps were produced as a result from the correlation between the bike measurements of the UHI for the city of Rotterdam (Heusinkveld et al., 2010), which was further extrapolated to the spatial and economic scenarios and to the climate scenarios (KNMI, 2009). The number of nights with temperatures above 20°C are higher in the area comprised between the Haagse Bos Park, Zuiderpark, Laakkwartier and Zorgvliet (Figure 5.5).

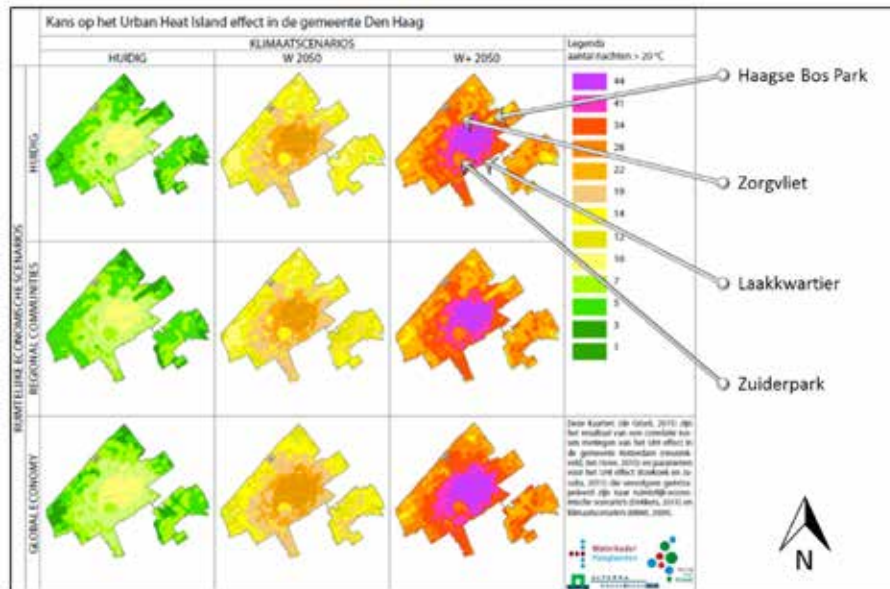


FIGURE 5.5 Night-time temperature in The Hague, the Netherlands. These maps (De Groot-Reichwein et al., 2014) are the result of a correlation between measurements of the UHI effect in the municipality of Rotterdam and parameters for the UHI, which are then extrapolated to spatial economic scenarios and climate scenarios.

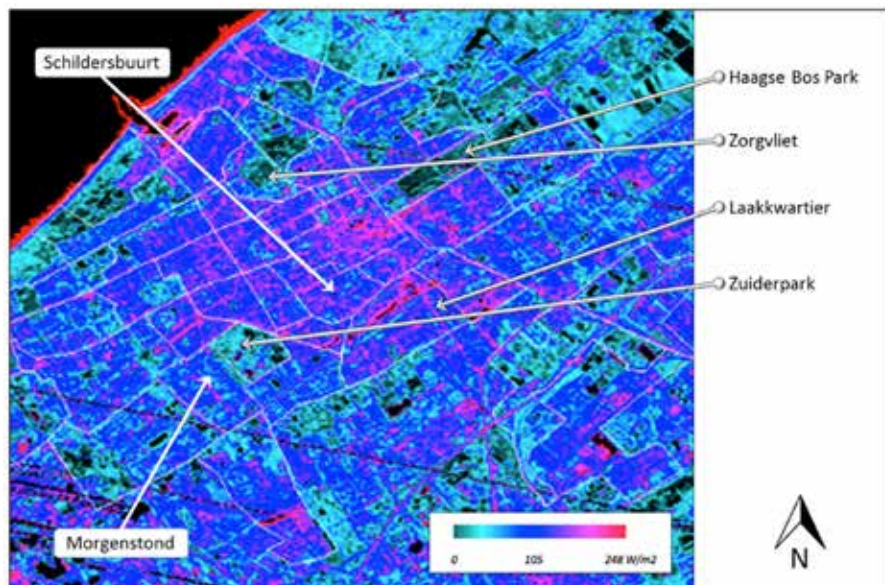


FIGURE 5.6 Storage heat flux map for The Hague, 16 July 2006. Landsat image (Courtesy of the U.S. Geological Survey. USGS/NASA Landsat) further processed with ENVI 4.7 and Atcor 2.3

Figure 5.6 presents the The Hague area comprising different neighbourhoods. For the city centre an average storage heat flux of  $92.82 \text{ W/m}^2$  was determined for the 16th of July 2006. For the Schildersbuurt area the average storage heat flux turned out to be  $85.08 \text{ W/m}^2$ . In contrast, in all scenarios the neighbourhood of Morgenstond has a lower average storage heat flux value than the area comprised between the Haagse Bos park, Zuiderpark, Laakkwartier and Zorgvliet also presents:  $68 \text{ W/m}^2$ . Morgenstond also presents less nights with temperatures above  $20^\circ\text{C}$ .

These examples, together with the visual comparison of the two images show that the maps depicting the prediction of nights with temperatures above  $20^\circ\text{C}$  are aligned with the results obtained when mapping the storage heat flux results during heat waves.

## § 5.4.2 Utrecht

Brandsma & Wolters (2012) have attempted to map the night-time UHI intensity for the city of Utrecht and its surroundings using high-resolution multi-day mobile observations for a single transect through the city for the period of March 2006-January 2009 (Figure 5.7).

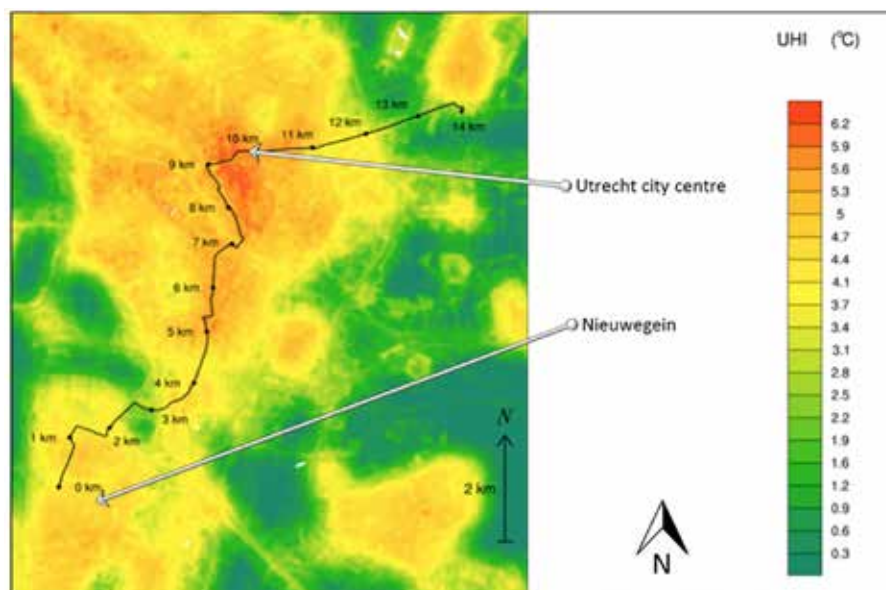


FIGURE 5.7 Spatial distribution of the maximum night-time UHI intensity for the city of Utrecht and its surroundings, from Brandsma & Wolters, 2012.

The areas with the highest night-time UHI – a temperature difference of around 6°C – are those in the North-Eastern part of the city centre, which also present the highest storage heat flux values on the 16th of July 2006 (Figure 5.8). As a reference, the average storage heat flux value in the city centre of Utrecht is 88.67 W/m<sup>2</sup>. In contrast, the area of Nieuwegein Noord, which is mapped with an UHI of around 4.3°C also has a considerably lower storage heat flux value: 65.8 W/m<sup>2</sup>.

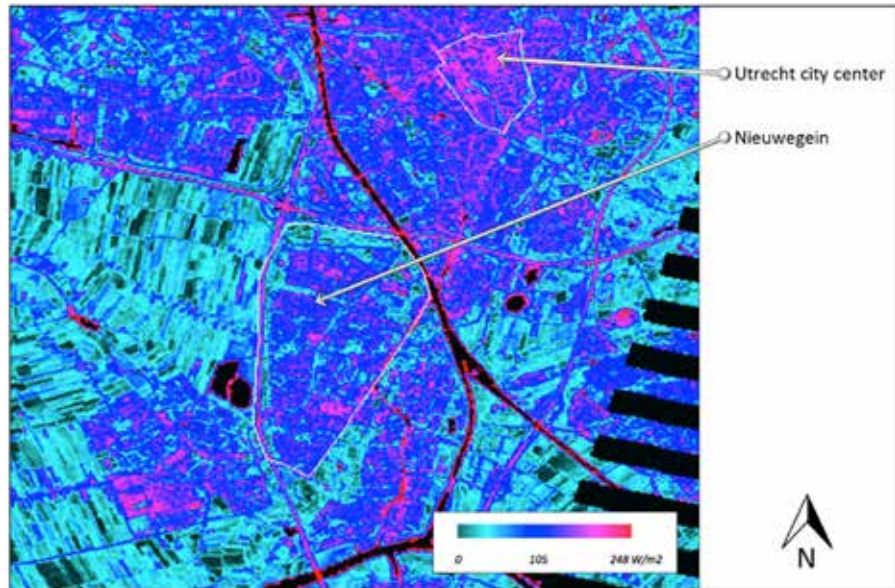


FIGURE 5.8 Storage heat flux map for Utrecht, 16 July 2006. Landsat image (Courtesy of the U.S. Geological Survey. USGS/NASA Landsat) further processed with ENVI 4.7 and Atcor 2.3

These examples, together with the visual comparison of the two images show that UHI mapping based on multi-day mobile observations seems aligned with the results obtained when mapping the storage heat flux results during a heat wave.

## § 5.5 Heat mitigation strategies in Dutch cities: relevant parameters

### § 5.5.1 Normalised Difference Vegetation Index (NDVI)

The NDVI is the Normalised Difference Vegetation Index which is used to quantify the vegetation density. Studies on land surface temperatures reveal that the imperviousness coefficient has a stronger linear relationship with land surface temperature values than with NDVI (Yuan et al., 2007), particularly in bare soil locations (Carlson et al., 1994). However, looking at the correlation between minimum air temperatures and NDVI we observe that the difference in urban and rural NDVI is linearly related with the difference in urban and rural minimum air temperatures (Gallo et al., 1993). The NDVI variation is more strongly related with the temperature variations than with the population data used in previous studies (Gallo et al., 1993). Moreover, several studies indicate that the heat fluxes can be expressed as a function of the vegetation indexes in rural environments (Choudury et al., 1994; Carlson et al., 1995). Therefore, NDVI can be considered as a relevant indicator for UHI studies.

- NDVI determination

The atmospheric correction of the satellite image was done in ATCOR 2/3 and the NDVI calculation was done in ENVI 4.7. using the index definition below:

#### FORMULA 5.5

$NDVI = (NIR - VIS) / (NIR + VIS)$  Where VIS is the surface reflectance in the red region (650 nm) and NIR is the surface reflectance in the near infrared region (850 nm).

- Results of NDVI analysis

The ATCOR-2/3 User Guide, version 8.2.1, serves as a reference for the different NDVI values corresponding to different surface types. For fully vegetated surfaces it establishes an NDVI of 0.78, for partially vegetated surfaces 0.33, for dark asphalt areas 0.09, and for bright concrete areas of 0.07 (Richter & Muller, 2005). In Switzerland, the studies carried out by Parlow revealed that the lowest NDVI values with less than 0.2 could be detected in the city centre of Basel and Mulhouse as well

as in some agricultural fields without vegetation during the particular time of the year when the satellite imagery was retrieved. The highest NDVI values reached values of up to 0.7 or more and these corresponded to forests and grassland areas (Parlow, 2003). In the hotspots of The Hague, Delft, Leiden, Gouda, Utrecht and Den Bosch, the average NDVI ranges from 0.31 to 0.39. Even though the average NDVI values is pretty similar for all the hotspots, the NDVI visualisation (Figure 5.9) suggests that there might be some consistent NDVI differences within the hotspots. These maps provide an indication of the areas with the lowest values, thus the areas where to increase the vegetation. Overall, the storage heat flux hotspots of these six cities are located in the historical city centres and it seems delicate to suggest increasing NDVI at street level without analysing in detail the design implications of such a mitigation proposal. The implementation of green roofs would therefore be the most plausible option. Several studies (Kurn et al., 1994; Sailor, 1995) estimate that the near-surface air temperatures over vegetated areas were 1°C lower than background air temperatures.

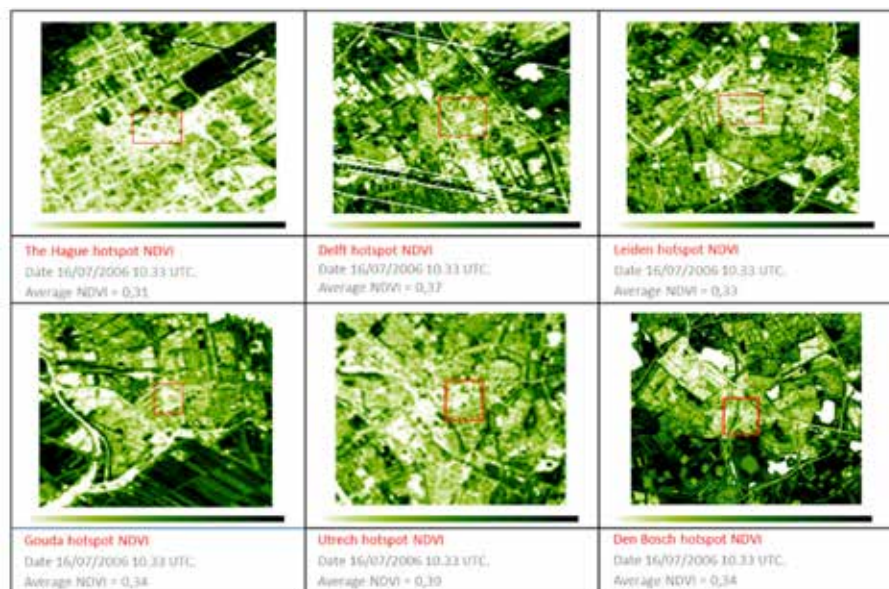


FIGURE 5.9 Normalised Difference Vegetation Index (NDVI) of the different Dutch cities. Landsat image (Courtesy of the U.S. Geological Survey. USGS/NASA Landsat) further processed with ENVI 4.7 and Atcor 2.3

## § 5.5.2 Land Surface Temperature (LST)

---

Areas with high diurnal LST represent areas whose heat can either be released to the atmosphere and/or to the interior of buildings within the day, or during the night, depending on the roof properties of the buildings assessed.

### – LST determination

The LST image has been obtained treating Landsat 5 TM imagery in ENVI 4.7, following the Yale Center for Earth Observation 2010 instructions to convert Landsat TM thermal bands into temperature. First the images are geometrically corrected and calibrated in ENVI 4.7, then the atmospherically corrected radiance is obtained applying Coll's equation (Coll et al., 2010):

#### FORMULA 5.6

$$CV R2 = [(CV R1 - L \uparrow) / \epsilon T] - [(1 - \epsilon) * (L \downarrow) / \epsilon]$$

Where:

CV R2 is the atmospherically corrected cell value as radiance.

CV R1 is the cell value as radiance

L  $\uparrow$  is upwelling radiance

L  $\downarrow$  is downwelling radiance

T is transmittance

E is emissivity (typically 0.95)

The transmittance as well as the upwelling and downwelling radiance can be retrieved from NASA's web page (NASA, 2014). Finally, the radiance can be converted into temperature (in Kelvin) as follows:

FORMULA 5.7

$$T = K2 / [\ln ((K1/CVR2) + 1)]$$

Where:

T is degrees Kelvin

CVR2 is the atmospherically corrected cell value as radiance.

K1 and K2 are prelaunch calibration constants

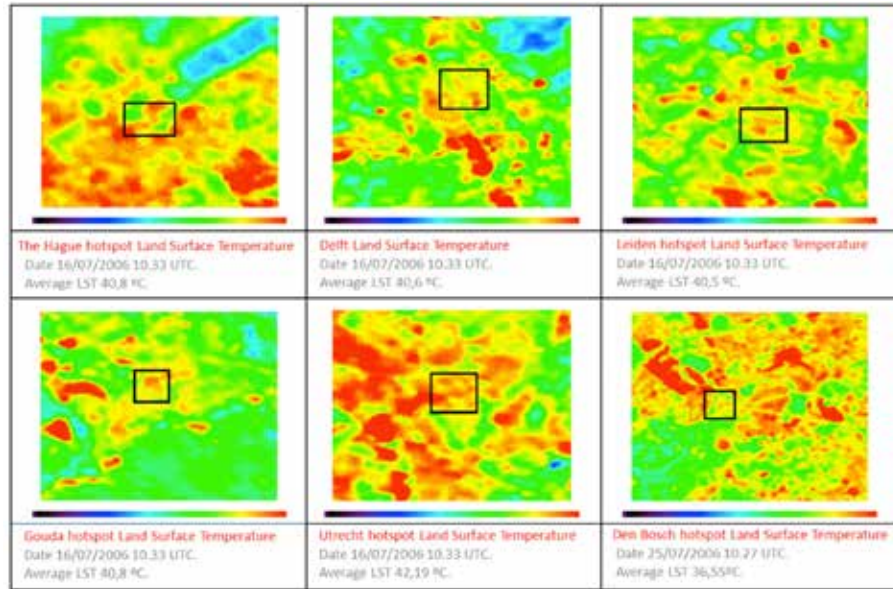


FIGURE 5.10 Land Surface Temperature (LST) of the different Dutch cities. Landsat image (Courtesy of the U.S. Geological Survey. USGS/NASA Landsat) further processed with ENVI 4.7 and Atcor 2.3

– Results of LST analysis

The land surface temperature images reveal that the storage heat flux hotspots do not necessarily present the highest diurnal LST values. As a matter of fact average land surface temperatures at 10:33 UTC in these city centers hotspots range from 36.55°C to 40.8°C (Figure 5.10), whereas other areas of the same cities present surface temperatures of up to 50°C. This is the case of The Brinckhorst, the Southern

Transvaal, Kerketuinen en Zichtenburg in The Hague, the case of Schieweg in Delft, of the industrial area close to the Zijkwartier in Leiden, to the Kromme Gouwe in Gouda or the industrial area between the Rietveldenweg and the Koenendelsweg in Den Bosch. These areas typically represent industrial areas that heat up very fast, but that also cool off very fast. This means that either the heat quickly penetrates into the buildings, or that it is quickly reflected back into the atmosphere. In the case of industrial buildings, which typically have bituminous sheet roofs, the heat retrieved by the roof is normally transferred to the interior of the buildings. If the industrial building does not need to preserve specific thermal conditions (storage use for example), it might not be worth it to implement any adaptation measure. If instead the building needs to preserve certain thermal conditions inside, the roof thermal behaviour could easily be improved by applying a reflective coating or surface coatings.

### § 5.5.3 Sky View Factor (SVF)

---

The sky view factor (SVF) was defined by Oke as the ratio of the amount of the sky seen from a given point to that potentially available (Oke, 1987). Its values range from 0 for full obstruction, to 1 for completely open areas. The average SVF in central parts of European cities ranges from 0.40 to 0.75, and the relationship with the nocturnal UHI was established by Oke (1981) and Park (1987), as follows:

#### FORMULA 5.8

$$\text{UHI}_{\text{max}} = 13.20 - 10 \cdot \text{SVF}$$

Where UHI max is the maximum UHI and SVF is the sky view factor.

These results are aligned with the studies carried out in Gothenburg (Sweden) and in Szeged (Hungary), which find a strong relationship between the SVF and the nocturnal UHI in calm, clear nights (Svensson, 2004; Unger, 2009). However, other investigations carried out in Germany reveal that the nocturnal UHI is not only affected by the horizon obstructions (SVF) but also by the thermal properties of the materials, and they only find a correlation between the long-wave radiation and the UHI, but not between the UHI and the SVF (Blankenstein & Kuttler, 2004). Many of these studies highlight the importance of the way the SVF is calculated, and at which height it is calculated.

- Sky View Factor determination

In the present study the calculation is done through the use of a SVF visualization tool developed by the Scientific Research Centre of the Slovenian Academy of Sciences and Arts (Zakšek et al., 2011) applied to the geographic Landsat image (Courtesy of the U.S. Geological Survey, USGS/NASA Landsat) of the concerned Dutch cities.

The Sky View Factor analysis allows to draw the city limits, to identify different urban structures within a city and to identify specific streets or urban areas with higher or lower sky view factors.

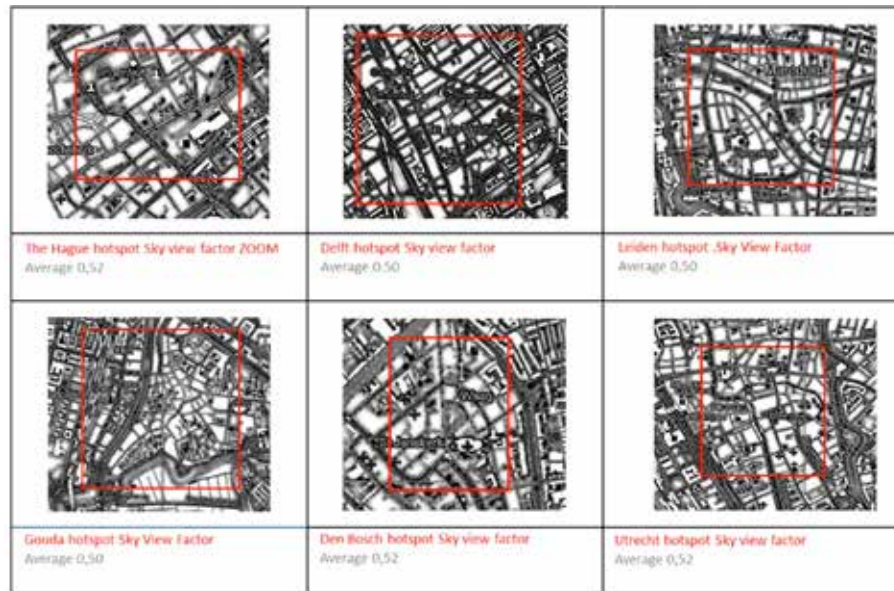


FIGURE 5.11 Sky View Factor (SVF) of the different Dutch cities

- Results of SVF analysis

The average Sky View Factor is almost the same for all hotspots (Figure 5.11). In the hotspots of the six analyzed cities, The Sky View Factor maps do not allow to identify specific hotspots within the urban areas. The Sky View Factor analysis allows to draw the city limits, to identify different urban structures within a city and to identify specific streets or urban areas with higher or lower sky view factors.

## § 5.5.4 Anthropogenic heat losses

---

Anthropogenic heat is not assessed in this paper. Average anthropogenic heat values in Europe range from 1.9 to 4.6 W/m<sup>2</sup> (Lindberg et al., 2013). These values increase in the urban environment reaching the 20 W/m<sup>2</sup> in cities as Berlin (Taha, 1997). Anthropogenic heat plays a role in the formation of UHI but they are not decisive in European cities.

## § 5.5.5 Coolspots and cool wind corridors

---

Just as hotspots, coolspots can be identified through the storage heat flux mapping. Coolspots are areas with the lowest storage heat flux values; if they are situated close to a hotspot, climate adaptation measures could be focused on transporting cool air from the coolspots to the hotspot, or on getting the heat from the hotspot dissolved in the coolspots. The calculation of the heat fluxes is done through different models for urban and for rural surfaces. In order to identify the coolspots surrounding the cities, the rural areas algorithm was applied.

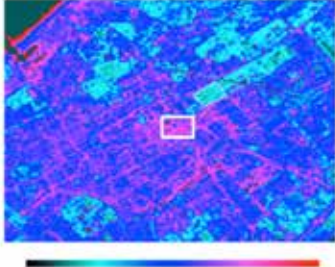
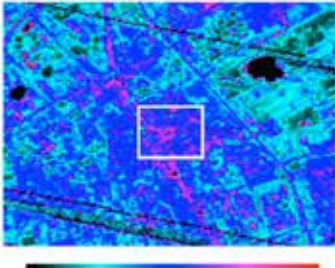
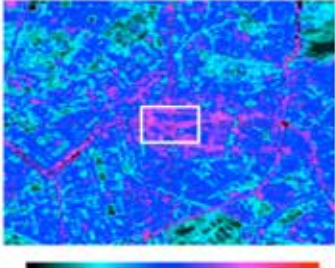
### – Coolspot determination

Storage heat flux is mapped in this study using Landsat 5 TM imagery and ATCOR 2/3 for the storage heat flux calculation. Since the coolspots often correspond to green areas, the ATCOR “rural” algorithm was applied for the estimation of the storage heat flux which employs a parametrization with the soil adjusted vegetation index (SAVI) (Choudury 1994, Carlson et al. 1995).

### FORMULA 5.9

$$G = 0.4 R_n (SAVI_m - SAVI) / SAVI_m$$

Where G is the storage heat flux, R<sub>n</sub> represents the net radiation, SAVI represents the Soil Sdjusted Vegetation Index and and SAVI<sub>m</sub> = 0.814 represents full vegetation cover.

	
<p><b>The Hague hotspot surrounding COOLSPOT</b> Closest coolspot: Haagse Bos.</p>	<p><b>The Hague hotspot cool paths.</b> Distance from hotspot to coolspot: CONNECTED</p>
	
<p><b>Delft hotspot surrounding COOLSPOT</b> Closest coolspot: Delftse Hout.</p>	<p><b>Delft hotspot cool paths</b> Distance from hotspot to coolspot: 580 m</p>
	
<p><b>Leiden hotspot surrounding COOLSPOT</b> Closest coolspot: South of Kanaalweg</p>	<p><b>Leiden hotspot wind paths.</b> Distance from hotspot to coolspot: 1300m</p>

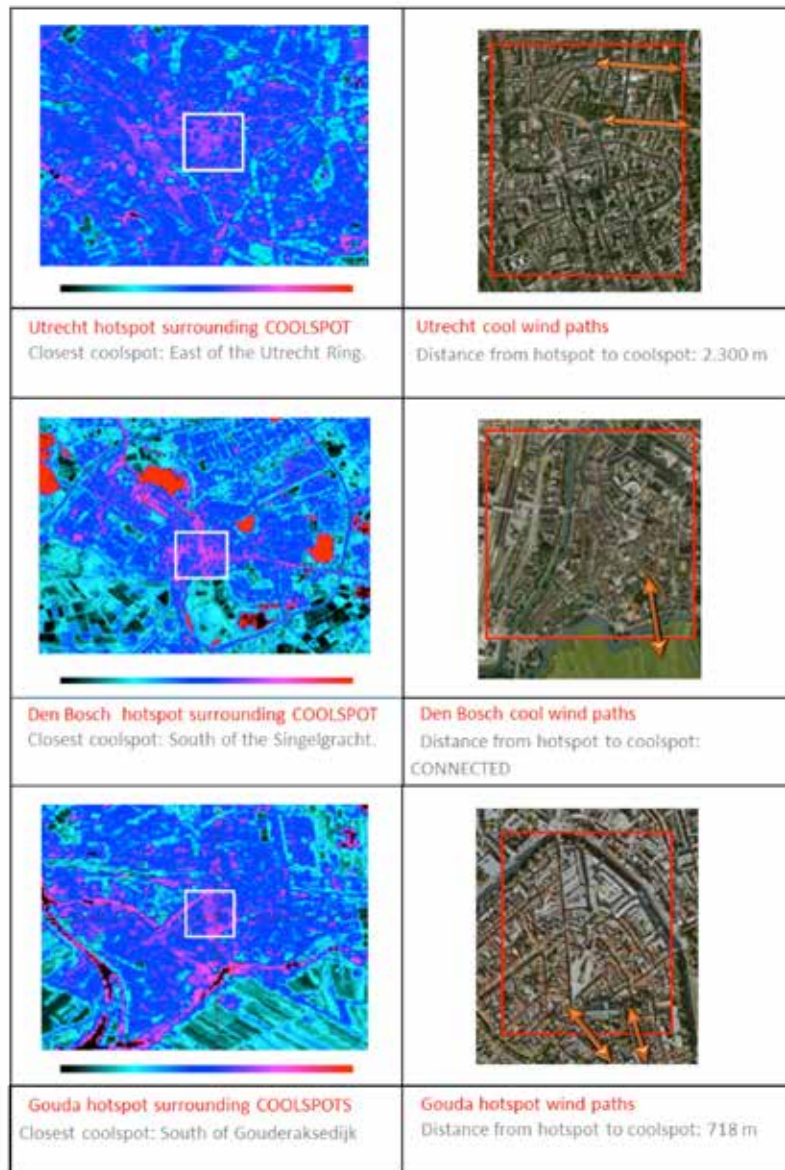


FIGURE 5.12 Coolspot analysis (Storage heat flux map for The Hague, Delft, Leiden, Utrecht, Den Bosch and Gouda 16 July 2006. Landsat image courtesy of the U.S. Geological Survey. USGS/NASA Landsat. further processed with ENVI 4.7 and Atcor 2.3) and wind corridor analysis of the different Dutch cities. Right column google earth imagery.

– Results of coolspot analysis

For the hotspot of the Hague, the coolspot identified is The Haagse Bos, in Delft the Delftse Hout, in Leiden the potential coolspot is located at around 1,300 m from the hotspot and corresponds to the greenfields to the South of the Kanaalweg and to the West of Zaalbergweg; in Gouda the greenfields to the South of the Gouderaksedijk (West of the Goudeseweg) although they are located 700 m away from the hotspot; in Utrecht the hinterland located to the East of the Utrecht Ring, in the areas of Fort Voordorp could also have a cooling effect on the hotspot although it is located at a distance of 2,300 m from it, in Den Bosch the greenfields located to the South of the Singelgracht and to the West of the Zuiderplas could represent a natural cooling source for the hotspot (Figure 5.12).

The identification of coolspots in the surrounding areas of the hotspots allows promoting the creation of cool wind corridors connecting the coolspots to the hotspots. In the case of The Hague, Delft, Gouda and Den Bosch the cooling sources are relatively close to the hotspots, and the efficiency of the cool corridor is almost guaranteed, as they would also benefit from the urban heat island plume. The adaptation measure in this case would consist of ensuring that the selected “cool corridors” (existing streets or canals, connecting the cool and hotspots) remain cleared from obstacles to ensure the maximum wind circulation during heat waves. The cases of Leiden and Utrecht probably require deeper wind analysis studies, as in both cases the cooling source is at a distance greater than 1,000 m from the hotspot.

## § 5.5.6 Albedo

---

In the urban environment it can be assumed that the storage heat flux represents 40% of the net radiation (Parlow, 1998). Increasing the surface reflectance (albedo) of the urban surfaces is considered as a means to reduce the UHI since it reduces the net short-wave (solar) radiation, thus reducing the total surface net radiation. Albedo is the index representing the surface reflectance. It indicates the fraction of short-wave radiation that is reflected from land surfaces into the atmosphere. When a surface albedo is 0 it doesn't reflect any radiation, and when it is 1 all the incoming radiation is reflected to the atmosphere.

Most US and European cities have albedos of 0.15 to 0.20 (Taha, 1997). A white surface with an albedo of 0.61 is only 5°C warmer than ambient air whereas conventional gravel with an albedo of 0.09 is 30°C warmer than air (Taha et al., 1992). Other studies carried out by Taha et al. reveal that increasing the surface albedo from 0.25 to 0.40 could lower the air temperature as much as 4°C (Taha et al., 1988), or even that an increase of 0.1 of the hotspot overall albedo reduces the UHI by 1°C. (Sailor 1995).

It is important to analyse albedo surface images, since vegetated areas or water bodies might present low albedo values, yet not necessarily have a negative impact on the UHI.

### – Albedo determination

The albedo of the six Dutch cities is mapped again using Landsat 5 TM imagery and importing it into ATCOR 2/3 for the albedo calculation (Figure 5.13).

In ATCOR 2/3 (Richter & Schlapfer, 2013) the wavelength-integrated surface reflectance (in a strict sense the hemispherical-directional reflectance), is used as a substitute for the surface albedo (bi-hemispherical reflectance) and it is calculated as:

#### FORMULA 5.10

$$a = \left[ \int_{0.3\mu\text{m}}^{2.5\mu\text{m}} \rho(\lambda) d\lambda \right] / \int_{0.3\mu\text{m}}^{2.5\mu\text{m}} d\lambda$$

Where  $a$  is the wavelength-integrated surface reflectance (used as a substitute for the surface albedo)

For Landsat 5 TM the following assumptions are made by ATCOR 2/3 for extrapolation:

Extrapolation for the 0.30-0.40  $\mu\text{m}$  region:  $\rho_{0.3-0.4\mu\text{m}} = 0.8 \rho_{0.45-0.50\mu\text{m}}$ .

Extrapolation for the 0.40-0.45  $\mu\text{m}$  region:  $\rho_{0.4-0.45\mu\text{m}} = 0.9 \rho_{0.45-0.50\mu\text{m}}$ .

The reflectance reduction factors in the blue part of the spectrum account for the decrease of surface reflection for most land covers (soils, vegetation). The extrapolation to longer wavelengths is computed as:

$\rho_{2.0-2.5\mu\text{m}} = 0.5 \rho_{1.6\mu\text{m}}$ , if  $\rho_{850}/\rho_{650} > 3$  (vegetation)

$\rho_{2.0-2.5\mu\text{m}} = \rho_{1.6\mu\text{m}}$ , else

Wavelength gap regions are supplemented with interpolation. The contribution of the 2.5 - 3.0  $\mu\text{m}$  spectral region can be neglected, since the atmosphere is almost completely opaque and absorbs all solar radiation.

Albedo: range 0-1000, scale factor 10, e.g., scaled albedo=500 corresponds to albedo=50%.



FIGURE 5.13 Albedo of the different Dutch cities. Landsat image (Courtesy of the U.S. Geological Survey, USGS/ NASA Landsat) further processed with ENVI 4.7 and Atcor 2.3

## § 5.6 Quantification of heat reduction through roof mitigation strategies.

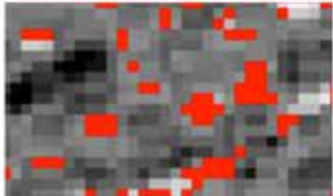
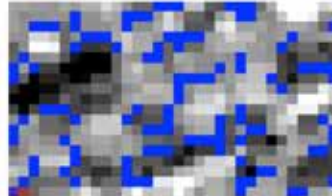
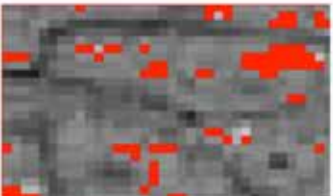
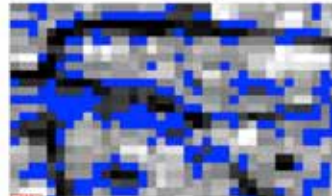
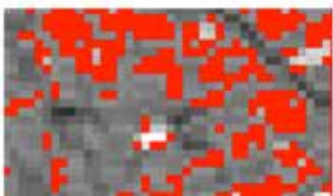
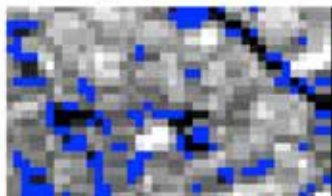
### § 5.6.1 Increasing the albedo

Delft, Leiden, Gouda, Utrecht and Den Bosch have a dense traditional 17th century inner-city with red ceramic roof tiles, brick street paving and canals. In order to improve the albedo in these hotspots, intervening on the brick street paving is provocative, as it is considered as part of the cultural heritage of these neighbourhoods. Instead, on the long run the existing roof tiles could be replaced by cool colour tiles, once the existing ones arrive to the end of their life cycle. Traditional tiles have albedo values that ranges from 18 to 22%, whereas the reflectance of orange cool tiles have a reflectance of around 50% (U.S. Environmental Protection Agency's Office of Atmospheric Programs). It is important to note that the market for these cool tiles is not consolidated yet, and

that one possible municipal or regional adaptation measure would be to encourage the production or the import of these innovative products.

As far as the bitumen flat roofs are concerned the primary cool roof option for moderate repair would be to install highly reflective coatings or surface treatments that can be applied to bituminous cap sheets, gravel, metal and various single ply materials. For more extensive repairs of flat roofs the primary option is the application of thermal insulation and highly reflective single ply membranes (or pre-fabricated sheets) generally glued to the entire roof surface.

The results of the estimation of the UHI reduction through the implementation of albedo (sloped and flat) (Figure 5.14) roof mitigation actions have an UHI reduction effect that ranges between 1.4°C and 3°C. (Figures 5.15, 5.16, 5.17, 5.18, 5.19 and 5.20) Considering that the max UHI values for the 95 percentile, calculated with the hobby meteorologists data (Hove et al., 2011) for the cities of The Hague, Delft and Leiden ranges from 4.8°C to 5.6°C implementing roof mitigation strategies seems an efficient way of reducing the UHI in these Dutch cities.

	
The Hague hotspot: Clay tile surface estimation 5,23 Ha	The Hague hotspot: Bitumen flat roof surface estimation 7,97 Ha
	
Leiden hotspot: Clay tile surface estimation 5,78 Ha	Leiden hotspot: Bitumen flat roof surface estimation 15 Ha
	
Delft hotspot: Clay tile surface estimation 26,46 Ha	Delft hotspot: Bitumen flat roof surface estimation 15,5 Ha

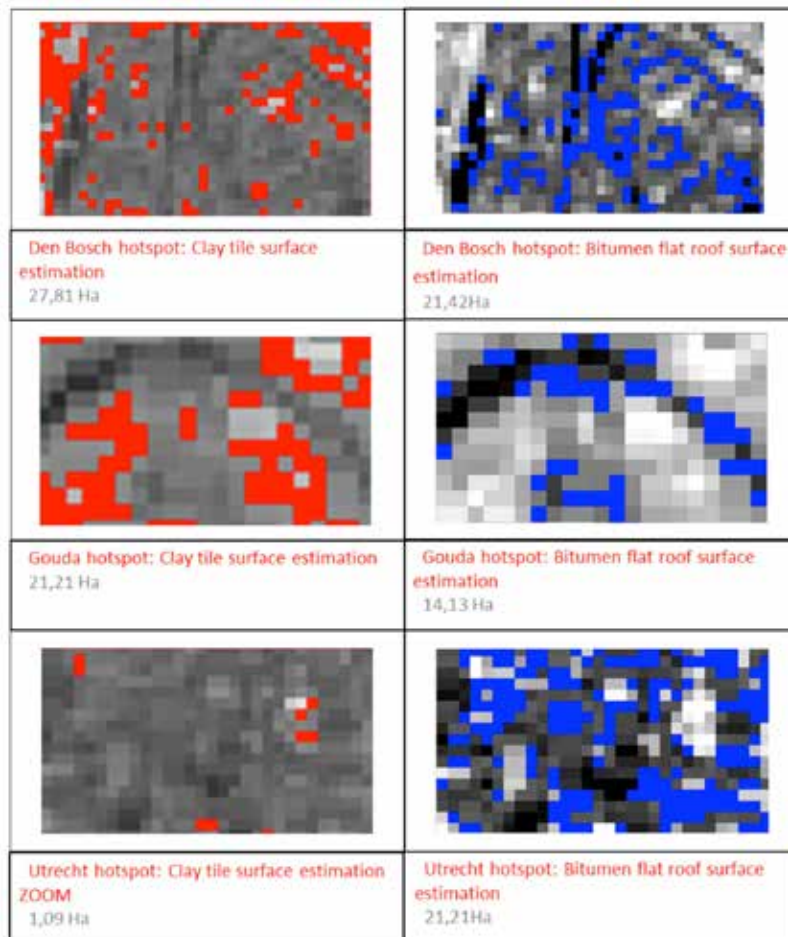


FIGURE 5.14 Albedo increase analysis of the different Dutch cities.

- The Hague: The UHI reduction estimation for several roof intervention scenarios can be seen in figure 5.15.

THE HAGUE					
Current situation		Hotspot surface (M <sup>2</sup> )	Hotspot average albedo	Estimated UHI max for 95 percentile	
		44,48	0,13	5,1	
Mitigation scenarios:					
Mitigation action 1: Next 20 years		Apply over flat between roofs (albedo 0.18 to 0.15) white coating (0.7) OR replace by white single-ply membrane (0.7)			
	surface	albedo of white coating or of single-ply membrane	Hotspot new average albedo	Average albedo increase	Estimated UHI max for 95 percentile
Area within hotspot with albedo ranging from 0.130 to 0.150 or highest estimation of flat bitumen roof surface		7,97	0,7	0,25	0,16
					4,31
					UHI reduction: 0,89
Mitigation action 2: Next 50 years		Replace all hotspot sloped roof clay tiles (albedo 0.18 to 0.22) by coloured tiles with cool pigments (albedo 0.3)			
	surface	albedo of coloured tiles with cool pigments	Hotspot average albedo	Average albedo increase	Estimated UHI max for 95 percentile
Area within hotspot with albedo ranging from 0.185 to 0.220 or highest estimation of sloped roof clay tile surface		3,23	0,3	0,18	0,04
					4,89
					UHI reduction: 0,41
Mitigation action 3 = 2: Next 50 years			Hotspot average albedo	Average albedo increase	Estimated UHI max for 95 percentile
			0,21	0,14	3,90
					UHI reduction: 1,40

FIGURE 5.15 Estimation of UHI reduction derived from the implementation of the roof mitigation strategies in the storage heat flux hotspot of The Hague

- Delft: The UHI reduction estimation for several roof intervention scenarios can be seen in figure 5.16.

DELFT					
Current situation		Hotspot surface (M <sup>2</sup> )	Hotspot average albedo	Estimated UHI max for 95 percentile	
		82,8	0,17	4,8	
Mitigation scenarios:					
Mitigation action 1: Next 20 years		Apply over flat between roofs (albedo 0.13 to 0.15) white coating (0.7) OR replace by white single-ply membrane (0.7)			
	surface	albedo of white coating or of single-ply membrane	Hotspot new average albedo	Average albedo increase	Estimated UHI max for 95 percentile
Area within hotspot with albedo ranging from 0.130 to 0.150 or highest estimation of flat bitumen roof surface		33,5	0,7	0,26	0,09
					5,91
					UHI reduction: 0,81
Mitigation action 2: Next 50 years		Replace all hotspot sloped roof clay tiles (albedo 0.18 to 0.22) by coloured tiles with cool pigments (albedo 0.3)			
	surface	albedo of coloured tiles with cool pigments	Hotspot average albedo	Average albedo increase	Estimated UHI max for 95 percentile
Area within hotspot with albedo ranging from 0.185 to 0.220 or highest estimation of sloped roof clay tile surface		26,89	0,3	0,21	0,08
					3,86
					UHI reduction: 0,94
Mitigation action 3 = 2: Next 50 years			Hotspot average albedo	Average albedo increase	Estimated UHI max for 95 percentile
			0,33	0,18	2,97
					UHI reduction: 1,83

FIGURE 5.16 Estimation of UHI reduction derived from the implementation of the roof mitigation strategies in the storage heat flux hotspot of Delft

- Leiden: The UHI reduction estimation for several roof intervention scenarios can be seen in figure 5.17.

LEIDEN						
Current situation		Hotspot surface (ha)	Hotspot average albedo	Estimated UHI max for 95 percentile		
		11,65	0,16	5,8		
Mitigation scenario:						
Mitigation action 1: Next 20 years						
Apply over flat bitumen roofs (albedo 0.13 to 0.15) white coating (0.7) OR replace by white single-ply membrane (0.5)						
Area within hotspot with albedo ranging from 0.130 to 0.150 or high-level estimation of flat bitumen roof surface		surface	albedo of white coating or of single-ply membrane	Hotspot new average albedo	Average albedo increase	Estimated UHI max for 95 percentile
		15	0,7	0,28	0,13	4,26
					<b>UHI reduction</b>	<b>1,54</b>
Mitigation action 2: Next 50 years						
Replace all hotspot sloped roof clay tiles (albedo 0.18 to 0.22) by coloured tiles with cool pigments (albedo 0.3)						
Area within hotspot with albedo ranging from 0.185 to 0.220 or high-level estimation of sloped roof clay tile surface		surface	albedo of coloured tiles with cool pigments	Hotspot average albedo	Average albedo increase	Estimated UHI max for 95 percentile
		5,78	0,3	0,18	0,03	5,27
					<b>UHI reduction</b>	<b>0,53</b>
Mitigation action 1 + 2: Next 50 years						
				Hotspot average albedo	Average albedo increase	Estimated UHI max for 95 percentile
				0,32	0,17	3,88
					<b>UHI reduction</b>	<b>1,92</b>

FIGURE 5.17 Estimation of UHI reduction derived from the implementation of the roof mitigation strategies in the storage heat flux hotspot of Leiden

- Gouda: The UHI reduction estimation for several roof intervention scenarios can be seen in figure 5.18.

GOUDA						
Current situation		Hotspot surface (ha)	Hotspot average albedo	Estimated UHI max for 95 percentile		
		33,8	0,17	5		
Mitigation scenario:						
Mitigation action 1: Next 10 years						
Apply over flat bitumen roofs (albedo 0.13 to 0.15) white coating (0.7) OR replace by white single-ply membrane (0.5)						
Area within hotspot with albedo ranging from 0.130 to 0.150 or high-level estimation of flat bitumen roof surface		surface	albedo of white coating or of single-ply membrane	Hotspot new average albedo	Average albedo increase	Estimated UHI max for 95 percentile
		4,13	0,7	0,24	0,07	4,29
					<b>UHI reduction</b>	<b>0,71</b>
Mitigation action 2: Next 50 years						
Replace all hotspot sloped roof clay tiles (albedo 0.18 to 0.22) by coloured tiles with cool pigments (albedo 0.3)						
Area within hotspot with albedo ranging from 0.185 to 0.220 or high-level estimation of sloped roof clay tile surface		surface	albedo of coloured tiles with cool pigments	Hotspot average albedo	Average albedo increase	Estimated UHI max for 95 percentile
		21,21	0,3	0,40	0,22	2,71
					<b>UHI reduction</b>	<b>2,29</b>
Mitigation action 1 + 2: Next 50 years						
				Hotspot average albedo	Average albedo increase	Estimated UHI max for 95 percentile
				0,47	0,30	2,07
					<b>UHI reduction</b>	<b>2,93</b>

FIGURE 5.18 Estimation of UHI reduction derived from the implementation of the roof mitigation strategies in the storage heat flux hotspot of Gouda

- Utrecht: The UHI reduction estimation for several roof intervention scenarios can be seen in figure 5.19.

UTRECHT						
Current situation		Hotspot surface (Ha)	Hotspot average albedo	Estimated UHI max for 95 percentile		
		60.8	0.34	5		
Mitigation scenario:						
Mitigation action 1: Next 10 years						
Apply over: flat bitumen roofs (albedo 0.13 to 0.15) white coating (0.7) OR replace by white single-ply membrane (0.7)						
		surface	albedo of white coating or of single-ply membrane	Hotspot new average albedo	Average albedo increase	Estimated UHI max for 95 percentile
Area within hotspot with albedo ranging from 0.130 to 0.150 or highest estimation of flat bitumen roof surface		25.21	0.7	0.34	0.20	3.06
					<b>UHI reduction:</b>	<b>0.93</b>
Mitigation action 2: Next 50 years						
Replace all hotspot sloped roof clay tiles (albedo 0.18 to 0.22) by coloured tiles with cool pigments (albedo 0.30)						
		surface	albedo of coloured tiles with cool pigments	Hotspot average albedo	Average albedo increase	Estimated UHI max for 95 percentile
Area within hotspot with albedo ranging from 0.180 to 0.220 or highest estimation of sloped roof clay tile surface		1.09	0.5	0.31	0.01	4.94
					<b>UHI reduction:</b>	<b>0.04</b>
Mitigation action 1 + 2: Next 50 years						
				Hotspot average albedo	Average albedo increase	Estimated UHI max for 95 percentile
				0.34	0.01	2.96
					<b>UHI reduction:</b>	<b>0.03</b>

FIGURE 5.19 Estimation of UHI reduction derived from the implementation of the roof mitigation strategies in the storage heat flux hotspot of Utrecht

- Den Bosch: The UHI reduction estimation for several roof intervention scenarios can be seen in figure 5.20.

DEN BOSCH						
Current situation		Hotspot surface (Ha)	Hotspot average albedo	Estimated UHI max for 95 percentile		
		133	0.17	5.1		
Mitigation scenario:						
Mitigation action 1: Next 10 years						
Apply over: flat bitumen roofs (albedo 0.13 to 0.15) white coating (0.7) OR replace by white single-ply membrane (0.7)						
		surface	albedo of white coating or of single-ply membrane	Hotspot new average albedo	Average albedo increase	Estimated UHI max for 95 percentile
Area within hotspot with albedo ranging from 0.130 to 0.150 or highest estimation of flat bitumen roof surface		21.42	0.7	0.26	0.08	4.03
					<b>UHI reduction:</b>	<b>0.07</b>
Mitigation action 2: Next 50 years						
Replace all hotspot sloped roof clay tiles (albedo 0.18 to 0.22) by coloured tiles with cool pigments (albedo 0.30)						
		surface	albedo of coloured tiles with cool pigments	Hotspot average albedo	Average albedo increase	Estimated UHI max for 95 percentile
Area within hotspot with albedo ranging from 0.180 to 0.220 or highest estimation of sloped roof clay tile surface		27.81	0.5	0.24	0.07	4.81
					<b>UHI reduction:</b>	<b>0.07</b>
Mitigation action 1 + 2: Next 50 years						
				Hotspot average albedo	Average albedo increase	Estimated UHI max for 95 percentile
				0.22	0.13	3.06
					<b>UHI reduction:</b>	<b>0.34</b>

FIGURE 5.20 Estimation of UHI reduction derived from the implementation of the roof mitigation strategies in the storage heat flux hotspot of Den Bosch

## § 5.7 Conclusions of UHI analysis of Dutch cities

### § 5.7.1 General findings

This study has two main objectives: the first one is to develop a method for the urban heat assessment based on the analysis of satellite imagery, and the second one is to develop some customised UHI adaptation guidelines for the cities of The Hague, Delft, Leiden, Gouda, Utrecht and Den Bosch.

- Satellite imagery analysis for UHI assessment:

Remote sensing can effectively be used to identify urban heat hotspots in areas where there is a lack of micro-measurements. Storage heat flux seems a relevant indicator for the identification of urban areas with a high tendency to accumulate heat. Storage heat flux can be mapped using Landsat 5 TM imagery and processing it in ATCOR 2/3 and ENVI 4.7.

The use of Landsat 5TM processed in ATCOR 2/3 and ENVI 4.7. also allows defining mitigation strategies to reduce urban heat in the identified hotspots. Mapping vegetation indexes, land surface temperature, coolspots and albedo, allows identifying areas where to implement more vegetation, areas where wind corridors (connecting hotspots to coolspots) could be created and areas where to increase the reflectance of the materials (to improve the albedo).

The same satellite imagery can be used to quantify the surface of bituminous flat roofs and of clay sloped roofs, in order to calculate a high level estimation of the mitigation effect of the increase of albedo of those surfaces.

- Customised UHI assessment for the cities of The Hague, Delft, Leiden, Gouda, Utrecht and Den Bosch:

The storage heat flux analysis for the 6 cities reveals that the hotspots have average storage heat flux values that range from 90 W/m<sup>2</sup> to 105 W/m<sup>2</sup>. See figure 5.21. Hotspot areas (areas with highest storage heat flux concentration) range from 30.8 ha in Gouda to 133 ha in Den Bosch.

Dutch cities	Surface of the hotspot <b>Ha</b>	Storage Heat Flux <b>W/m<sup>2</sup></b>	<b>NDVI</b>	<b>LST <b>°C</b></b>	<b>Albedo</b>	<b>Average %VI</b>	<b>Sensible heat</b>	<b>Coolspot edge flux (distance to hotspot m)</b>
The Hague	44,5	101	0,31	40,8	0,15	0,5	156	26 (connected)
Delft	92,8	91,2	0,37	40,6	0,17	0,5	76,3	47 (188)
Leiden	61,7	103	0,33	40,5	0,15	0,5	173,6	40 (1300)
Gouda	30,8	96,7	0,34	40,8	0,17	0,5	168,4	41 (718)
Utrecht	60,8	94,6	0,39	42,2	0,14	0,5	184,4	47,7 (2300)
Den Bosch	133	104,1	0,34	36,6	0,17	0,5	138,8	58,7 (connected)

**FIGURE 5.21** Analysis of storage heat flux hotspots in the cities of The Hague, Delft, Leiden, Gouda, Utrecht and Den Bosch. It is important to highlight that the storage heat flux images and values might be distorted in areas covered by water, since the algorithm used by ATCOR for the storage heat flux calculation is based on Parlow's equation  $G=0.4 R_n$ , which is a valid assumption for urban areas but not for water surfaces

The hotspots in all cities correspond with the old city centres of each city, except for the case of The Hague, where it is not related to a homogeneous urban structure. The hotspots of Delft, Leiden, Gouda, Utrecht and Den Bosch, correspond to the dense traditional 17th century Dutch neighbourhoods with red ceramic roof tiles, brick street paving, and canals. These are typical dwelling neighbourhoods with commercial premises in the ground floor, characterised by a high quality of life. These inner-city areas belong to representative neighbourhoods with very intense street activity (commercial, leisure, and touristic). In contrast, the hotspot of the city of The Hague corresponds with an area with bituminous flat roofs and asphalt paving.

The analysis of the vegetation index maps allows to identify areas where the average value is below 0.2, and that could eventually benefit from an increase of vegetation, whether that vegetation is implemented at street level or at roof level. The coolspot analysis reveals that the in the cities of The Hague, Delft, Gouda and Den Bosch the distance between hotspots and coolspots is below 1,000m, which suggests that the creation of wind corridors could efficiently contribute to the mitigation of the urban heat, and the analysis of the albedo maps allows to identify the areas that could benefit from an increase of the surface reflectance.

The quantification of the bituminous flat roofs and clay sloped roofs, reveals that increasing the albedo of both type of surfaces could help reduce the UHI from 1.4 to 3 °C in the analysed cities.

## § 5.7.2 Implications of the work

Using remote sensing for UHI assessment allows cities to identify the areas where to concentrate their mitigation efforts. Further, it provides them with an overview of different adaptation alternatives (vegetation, albedo, wind corridors,...) to help

combine the climate mitigation efforts with other urban planning priorities, and finally it facilitates the quantification of the measures mitigation effect. Cities often only need this kind of high level overview to start taking urban heat into consideration in their urban plans. Deeper climatological studies can always be carried out to provide a more detailed assessment where needed.

The simultaneous analysis of several cities can help increase their awareness, and develop parallel mitigation plans, which can benefit from one another, sharing not only scientific and applied knowledge, but also implementation and management strategies. Remote sensing is specifically suited to carry out the analysis of several cities at the same time due to the large size of its scenes.

### § 5.7.3 Replicability of the study

---

The study can be replicated with a basic remote sensing and climatological knowledge and requires a certain command of the two main software utilised (ENVI 4.7 and ATCOR 2.3). One critical item is the selection of the satellite imagery, which should preferably be retrieved during a heat wave, and on a cloudless and windless day.

The satellite imagery used for this study is Landsat 5 TM however the same exercise can be performed with finer resolution satellite imagery, thus obtaining more accurate results.

### References

---

- ASAEDA, T.; CA, T.V.; WAKE, A. Heating of paved grounds and its effect on the near surface atmosphere: Exchange processes at the land surface for a range of space and time scales. Proceedings Yokohama Symposium, July 1993. IAHS Publ. 212, International Association of Hydrological Sciences, 1993. 181–187.
- ASRAR, G. Theory and Applications of Optical Remote Sensing. Wiley Series in Remote Sensing and Image Processing, Wiley-Interscience, 1989.
- BAUDOUIN, Y.; LEFEBVRE S. Urban heat island mitigation measures and regulations in Montréal and Toronto. Canada Mortgage and Housing Corporation, 2014.
- BLANKENSTEIN, S.; KUTTLER W. Impact of street geometry on downward longwave radiation and air temperature in an urban environment. In Meteorologische Zeitschrift, 15, 2004. 373-379.
- BECHTEL, B. Multitemporal Landsat data for urban heat island assessment and classification of local climate zones. Urban Remote Sensing Event (JURSE), 2011.
- BRANDSMA, T.; WOLTERS, D. Measurement and Statistical Modeling of the Urban Heat Island of the City of Utrecht, the Netherlands. In Journal of Applied Meteorology and Climatology, 51, 2012. 1046–1060.
- CAO, L.; LI, P.; ZHANG, L.; CHEN, T. Remote sensing image-based analysis of the relationship between urban heat island and vegetation fraction. The international Archives of Photogrammetry, remote sensing and spatial information sciences, vol XXXVII, part B7, 2008.

- CARLSON, T. N.; CAPEHART, W. J.; GILLIES, R. R. A new look at the simplified method for remote sensing of daily evapotranspiration. In *Remote Sensing of Environment*, 54.2, 1995. 161-167.
- CARLSON, T.N.; DODD, J.K.; BENJAMIN, S.G.; COOPER J.N. Satellite estimation of the surface energy balance, moisture availability and thermal inertia. In *Journal of Applied Meteorology*, 20, 1981. 67-87.
- CARLSON, T. N.; GILLIES, R. R.; PERRY, E. M. A method to make use of thermal infrared temperature and NDVI measurements to infer surface soil water content and fractional vegetation cover. In *Remote Sensing Reviews*, 9, 1994. 161-173.
- CHOUDHURY, B.J.; AHMED, N.U.; IDSO, S.B.; REGINATO, R.J.; DAUGHTRY, C.S.T. Relations between evaporation coefficients and vegetation indices studied by model simulations. In *Remote Sensing Environment*, 50, 1994. 1-17.
- COLL, C.; GALVE, J. M.; SÁNCHEZ, J. M.; CASELLES, V. Validation of Landsat-7/ETM+ Thermal-Band Calibration and Atmospheric Correction With Ground-Based Measurements. *IEEE Trans. In Geoscience Remote Sensing*, vol. 48.1, 2010. 547-555.
- CLIMATE ADAPTATION FOR RURAL AREAS. (Accessed June 2015). URL: <http://www.knowledgeforclimate.nl/ruralareas/researchthemeruralareas/consortiumclimateadaptationforconsortiu>.
- CLIMATE PROOF CITIES (CPC). (Accessed January 2014). URL: <http://knowledgeforclimate.climateresearchnetherlands.nl/climateproofcities/background-information>
- DE GROOT-REICHWEIN, M.A.M.; VAN LAMMEREN, R.J.A.; GOOSEN, H.; KOEKOEK, A.; BREGT, A.K.; VELLINGA P. Urban heat indicator map for climate adaptation planning. In *Mitigation and Adaptation Strategies for Global Change*, 2014.
- DOLL, D.; CHING, J. K. S.; KANESHIRO, J. Parametrization of subsurface heating for soil and concrete using net radiation data. In *Boundary-Layer Meteorology*, 10, 1985. 351-372.
- DOUSSET, B.; GOURMELON, F.; LAALDI, K.; ZEGHNOUN, A.; GIRAUDET, E.; BRETIN, P.; MAURI, E.; VANDENTORREN, S. Satellite monitoring of summer heat waves in the Paris metropolitan area. In *International Journal of Climatology*, 31, 2011. 313-323.
- EXELISVIS. <https://www.exelisvis.com/>
- GALLO, K. P.; MCNAB, A. L.; KARL, T. R.; BROWN, J. F. ; HOOD, J. J.; TARPLEY, J. D. The use of NOAA AVHRR data for assessment of the urban heat island effect. In *Journal of Applied Meteorology*, 32.5, 1993. 899-908.
- GARSSSEN, J.; HARMSSEN, C.; DE BEER, J. The effect of the summer 2003 heat wave on mortality in the Netherlands. In *Eurosurveillance*, 10. 7, 2005. 165-167.
- HEUSINKVELD, B.G.; HOVE, L.W.A.; VAN JACOBS, C.M.J.; STEENEVELD, G.J.; ELBERS, J.A.; MOORS, E.J.; HOLTSLAG, A. A. M. Use of a mobile platform for assessing urban heat stress in Rotterdam. Wageningen UR, 2010.
- HOEVEN, F. D.; WANDL, A. Amsterwarm. Gebiedstypologie warmte-eiland Amsterdam. Delft, Nederland: TU Delft, Faculty of Architecture, 2013.
- HOVE, L.W.A.; STEENEVELD, G.J.; JACOBS, C.M.J.; HEUSINKVELD, B.G.; ELBERS, J.A.; MOORS, E.J.; HOLTSLAG, A.A.M. Exploring the Urban Heat Island Intensity of Dutch Cities. Alterra report 2170. Wageningen, Netherlands, 2011.
- KLOK, L.; BROEKE, H.T.; HARMELEN, T.V.; VERHAGEN, H.; KOK, H.; ZWART, S. Ruimtelijke verdeling en mogelijke oorzaken van het hitte-eiland effect. Utrecht: TNO Bouw en Ondergrond, 2010.
- KNOWLEDGE FOR CLIMATE. (Accessed June 2015). URL: <http://www.knowledgeforclimate.nl/programme/background>
- KONINKLIJK NEDERLANDS METEOROLOGISCH INSTITUUT (KNMI). 2050 Climate Scenarios. KNMI, De Bilt, 2006. Available online: [http://www.knmi.nl/climatescenarios/#Inhoud\\_0](http://www.knmi.nl/climatescenarios/#Inhoud_0)
- KOOPMANS, S. First assessment of the urban heat island in the Netherlands. Exploring urban heat and heat stress in the Netherlands, using observations from hobby meteorologists. BSc Thesis Wageningen University, 2010. 35.
- KURN, D.; BRETZ, S.; HUANG, B.; AKBARI, H. The Potential for Reducing Urban Air Temperatures and Energy Consumption through Vegetative Cooling. ACEEE Summer Study on Energy Efficiency in Buildings, 31. American Council for an Energy Efficient Economy, Pacific Grove, California, 1994.
- LINDBERG, E.; HOLLAUS, M.; MÜCKE, W.; FRANSSON, J.E.S.; PFEIFER, N. Detection of lying tree stems from airborne laser scanning data using a line template matching algorithm. *Proceedings of ISPRS Annals II-5/W2*. Antalya, Turkey, November 11-13, 2013.
- LIU, L.; ZHANG, Y. Urban Heat Island Analysis Using the Landsat TM Data and ASTER Data: A case study in Hong Kong. In *Remote Sensing of Environment*, 3, 2011. 1535-1552.

- MEEHL, G.A.; TEBALDI, C. More Intense, More Frequent, and Longer Lasting Heat Waves in the 21st Century. In *Science*, 305 (5686), 2004. 994-997.
- MORRIS, C.J.G.; SIMMONDS, I.; PLUMMER, N. Quantification of the influences of wind and cloud on the nocturnal Urban Heat Islands of a large city. In *Journal of Applied Meteorology*, 40, 2001. 169-182. NASA (accessed 2014). URL : <http://atmcorr.gsfc.nasa.gov/>
- NICHOL, J.; WONG, M. Modeling urban environmental quality in a tropical city. In *Landscape and urban planning*, 2004.
- ODINDI, J.O.; BANGAMWABO, V.; MUTANGA, O. Assessing the value of urban green spaces in mitigating multi-seasonal urban heat using Modis land surface temperature (LST) and Landsat 8 data. In *International Journal of Environmental Resilience*, 9 (1), 2015. 9-18.
- OKE, T.R. City size and urban heat island. In *Atmospheric Environment*, vol 7, 8, 1973. 769-779.
- OKE, T.R. Canyon geometry and the nocturnal urban heat island: comparison of scale model and field observations. In *Journal of Climatology*, 1, 1981. 237-254.
- OKE, T.R. The energetic basis of the urban heat island. In *Quarterly journal of the Royal Meteorological Society*, 108 (455), 1982. 1-24.
- OKE, T.R. *Boundary Layer Climates*. 2nd edition, Routledge, 1987. 262-303.
- OKE, T. Urban environments. In *Surface Climates of Canada*. Mc Gill-Queen's University Press, Montréal, 1997. 303-327.
- ONISHI, A.; CAO, X.; ITO, T.; SHI, F.; IMURA, H. Evaluating the potential for urban heat-island mitigation by greening parking lots. In *Urban Forestry and Urban Greening*, 9, 2010. 323-332.
- PARK, H.S. Variations in the urban heat island intensity affected by geographical environments. *Environmental Research Center Papers*, 11. University of Tsukuba, Ibaraki, 1987.
- PARLOW, E. The Urban Heat Budget Derived from Satellite Data. In *Geographica Helvetica*, 58, 2003.
- PARLOW, E. Net radiation of urban areas. *Proceedings of the 17th EARSeL Symposium on Future Trends in Remote Sensing*, Lyngby, Balkema, Rotterdam, Denmark, 17-19 June 1997. 221-226.
- PRICE, J.C. Assessment of the urban heat island effect through the use of satellite data. In *Monthly Weather Review*, 107.11, 1979. 1554-1557.
- RAJASEKAR, U.; WENG, M. Spatio-temporal modelling and analysis of urban heat islands by using Landsat TM and ETM+ imagery. In *International Journal of Remote Sensing*, 30:13, 2009. 3531-3548.
- RICHTER, R.; MULLER, A. De-shadowing of satellite/airborne imagery. In *International Journal Remote Sensing*, volume 26, 2005. 3137-3148.
- RICHTER, R.; SCHLAPFER, D. Atmospheric/Topographic Correction for Satellite Imagery. ATCOR-2/3 User Guide, version 8.2.1, 2013. <http://www.rese.ch/products/atcor/atcor3/>
- RIGO, G.; PARLOW, E. Modelling the ground heat flux of an urban area using remote sensing data. In *Theoretical and Applied Climatology*, 90, 2007. 185-199.
- ROSENZWEIG, C.; SOLECKI, W.D.; SLOSBERG, R.B. Mitigating New Yorks city's heat island with urban forestry, living roofs, and light surfaces. *New York City regional heat island initiative final report*. New York State Energy Research and Development Authority (NYSERDA), 2006.
- ROTH, M.; OKE, T.; EMERY, W.J. Satellite-Derived Urban Heat Islands from Three Coastal Cities and the Utilization of such Data in Urban Climatology. In *International Journal of Remote Sensing*, 10, 1989. 1699-1720.
- SAILOR, D.J. Simulated Urban Climate response to modification in surface albedo and vegetative cover. In *Journal of Applied Meteorology*, 34 (7), 1995. 1694-1704.
- SCHAR, C.; JENDRITZKY, G. Climate Change: Hot news from summer 2003. In *Nature*, 432, 2004. 559-560.
- STEENEVELD, G.J.; KOOPMANS, S.; HEUSINKVELD, B.G.; VAN HOVE, L.W.A.; HOLTSLAG, A.A.M. Quantifying urban heat island effects and human comfort for cities of variable size and urban morphology in the Netherlands. In *Journal of Geophysical Research*, 116, 2011.
- SVENSSON, M.K. Sky view factor analysis – implications for urban air temperature differences. In *Meteorological Applications*, 11-3, 2004. 201-211.
- TAHA, H. Urban climates and heat islands: albedo, evapotranspiration, and anthropogenic heat. In *Energy and Buildings*, 25, 1997. 99-103.
- TAHA, H.; AKBARI, H.; ROSENFELD, A.H.; HUAND, Y.J. Residential cooling loads and the urban heat island: The effects of albedo. In *Building and Environment*, 23, 1988. 271-283.
- TAHA, H.; AKBARI, H.; SAILOR, D.; RITSCHARD, R. Causes and effects of heat islands: sensitivity to surface parameters and anthropogenic heating. *Lawrence Berkeley Lab. Rep. 29864*, Berkeley, CA, 1992.
- UNGER, J. Some aspects of the urban heat island phenomenon. Thesis for the MTA doctor's degree, 2009.

- UNITED STATES ENVIRONMENTAL PROTECTION AGENCY (US EPA). Office of Atmospheric Programs. Reducing Urban Heat Islands: Compendium of Strategies Cool Roofs. Climate Protection Partnership Division. URL: <http://www.epa.gov/hiri/resources/pdf/CoolRoofsCompendium.pdf>
- UNITED STATES ENVIRONMENTAL PROTECTION AGENCY (US EPA). Office of Atmospheric Programs. Reducing Urban Heat Islands: Compendium of Strategies Cool Pavements. Climate Protection Partnership Division. URL: <http://www.epa.gov/hiri/mitigation/pavements.htm>
- UNITED STATES GEOLOGICAL SURVEY (USGS). Earth Resources Observation and Science Center (EROS) (consulted 2013). URL: <http://glovis.usgs.gov/>
- UNO, I.; WAKAMATSU, I.; UEDA, H.; NAKAMURA, A. An observational study of the structure of the nocturnal urban boundary layer. In *Boundary Layer Meteorology*, 45, 1988. 59–82.
- VOOGT, J. Urban Heat Island. *Encyclopedia of Global Environmental Change*, vol. 3, 2002.
- YUAN, F.; BAUER, M.E. Comparison of impervious surface area and Normalised difference vegetation as indicators of surface urban heat island effects in Landsat imagery. In *Remote Sensing of Environment*, 106, 2007. 375-386.
- ZAKSEL, K.; OŠTIR, K.; KOKALJ, Ž. Sky-View Factor as a Relief Visualization Technique. In *Remote Sensing of Environment*, 3, 2011. 398-415.

